This paper is available on line at http://www.mcponline.org

Proteome Analysis of Distinct Developmental Stages of Human Natural Killer (NK) Cells[S]

Maxi Scheiter‡, Ulrike Lau‡, Marco van Ham‡, Björn Bulitta‡, Lothar Gröbe§, Henk Garritsen¶, Frank Klawonn‡‖, Sebastian König‡, and Lothar Jänsch‡*

The recent Natural Killer (NK) cell maturation model postulates that $CD34^+$ hematopoietic stem cells (HSC) first develop into $CD56^{bright}$ NK cells, then into $CD56^{dim}CD57^-$ and finally into terminally maturated $CD56^{dim}CD57^+$. The molecular mechanisms of human NK cell differentiation and maturation however are incompletely characterized. Here we present a proteome analysis of distinct developmental stages of human primary NK cells, isolated from healthy human blood donors. Peptide sequencing was used to comparatively analyze $CD56^{bright}$ NK cells *versus* $CD56^{dim}$ NK cells and $CD56^{dim}CD57^-$ NK cells *versus* $CD56^{dim}CD57^+$ NK cells and revealed distinct protein signatures for all of these subsets. Quantitative data for about 3400 proteins were obtained and support the current differentiation model. Furthermore, 11 donor-independently, but developmental stage specifically regulated proteins so far undescribed in NK cells were revealed, which may contribute to NK cell development and may elucidate a molecular source for NK cell effector functions.

Among those proteins, S100A4 (Calvasculin) and S100A6 (Calcyclin) were selected to study their dynamic subcellular localization. Upon activation of human primary NK cells, both proteins are recruited into the immune synapse (NKIS), where they colocalize with myosin IIa. ***Molecular & Cellular Proteomics 12: 10.1074/mcp.M112.024596, 1099–1114, 2013.***

Natural killer (NK)[1] cells are large granular lymphocytes that provide a first innate immune defense. They are able to kill virus-infected and transformed cells and furthermore release cytokines and chemokines to activate adaptive immune cells (1, 2).

The balance of signals from activating and inhibitory NK cell surface receptors tightly regulates NK cell activity. Activated NK cells release lytic granules through a process called degranulation. Therefore, NK cell cytotoxicity requires the formation of the F-actin-rich NK immune synapse (NKIS) and the transport of Perforin-containing lytic granules to the NKIS. Furthermore, this process requires granule-associated MYH9 protein (non-muscle Myosin IIa) mediating the interaction of granules with F-actin at the NKIS (3–5), leading to lytic granule exocytosis. Whereas related phenotypes and functional properties are well characterized, the underlying regulatory protein network mediating differentiation, cytokine release, and cytotoxicity, is still incomplete.

NK cells are defined by the expression of the surface molecule CD56 (NCAM1) and the absence of the T cell receptor (TCR) associated protein CD3 and can be further subdivided into subsets (6, 7). CD56 expressing cells originate from $CD34^+$ HSCs. Notably, the commitment to the NK lineage includes discrete steps from HSC to cells, expressing high CD56 levels ($CD56^{bright}$) (8, 9), which act immune regulatory by the release of various cytokines. NK cells with low CD56-expression ($CD56^{dim}$) predominantly constitute cytotoxic responses (10, 11). Contact of CD56 (NCAM1) with fibroblasts (12) and neutrophils (13) supports the differentiation process from $CD56^{bright}$ to $CD56^{dim}$ NK cells. The progression of early differentiation steps is proven by telomere length investigation (14) and early presence in blood after HSC transplantation (HSCT) (14, 15). Indeed, $CD56^{dim}$ NK cells are able to change their phenotypic properties, which can be correlated with continued differentiation throughout their whole lifespan (15–18). CD57 was determined to be a senescence marker in T cells (19). Recent studies determined $CD57^+$ NK cells as a fully mature NK cell subset among the $CD56^{dim}$ NK cell pop-

From the ‡Research Group Cellular Proteomics, Helmholtz Centre for Infection Research (HZI), Inhoffenstraβe 7, D-38124 Braunschweig, Germany, §Department of Experimental Immunology, Helmholtz Centre for Infection Research (HZI), Inhoffenstraβe 7, D-38124 Braunschweig, Germany, ¶Institute for Clinical Transfusion Medicine, Städtisches Klinikum Braunschweig gGmbH, Celler Str. 38 , D-38114 Braunschweig, Germany, ‖Department of Computer Science, Ostfalia University of Applied Sciences, Salzdahlumer Str. 46/48, D-38302 Wolfenbuettel, Germany

Received October 8, 2012, and in revised form, January 8, 2013
Published, MCP Papers in Press, January 13, 2013, DOI 10.1074/mcp.M112.024596

[1] The abbreviations used are: NK, natural killer; CD56, NK cell marker; NCAM1, neural cell adhesion molecule; CD57, senescence marker in T and NK cells (HNK-1 or Leu-7); CMV, cytomegalovirus; CPDA-1, anticoagulant , containing citric acid, sodium citrate, monobasic sodium phosphate and dextrose; CTLs, cytotoxic T lymphocytes; FDR, false discovery rate; HLA, self-human leukocyte antigen; HSC, hematopoietic stem cell; iTRAQ, isobaric tags for relative and absolute quantification in mass spectrometry; KIR, killer immunoglobulin-related receptors in NK cells; LC-MS/MS, liquid-chromatography coupled with peptide sequencing (mass spectrometry); MAD, median absolute deviation from the median; NKIS, NK cell immune synapse; RF, regulation factor.

ulation (CD56^{dim}CD57^{+} and CD56^{dim}CD57^{-}). Furthermore, the NK cell differentiation process is characterized by a reversible loss of NKG2A in parallel with an irreversible acquisition of KIRs and CD57 (15).

Furthermore, CD57^{+} NK cells are characterized by a specialized phenotype that includes increased CD16- and Perforin-expression, reduced responsiveness to cytokines and decreased proliferation capacity. CD57 is mostly studied in the context of NK cell education that runs in parallel but uncoupled from NK cell differentiation (15, 17, 18). The NK cell education process encompasses the acquisition of activating and inhibitory surface receptors, like KIRs, which in turn interact with HLA class I ligands, *e.g.,* during viral infections (19, 20). CD57^{+} NK cells can recognize cytomegalovirus (CMV) and developed memory effects toward this virus (21, 22). Likewise, an expansion of the CD57^{+} NK cell population is observed during Hantavirus (24), Chikungunya virus (25), and HIV-1 (16), but not during HSV-2 (26) infections. Recently, Lanier and colleagues showed that IL-12 is indispensable for NK cell expansion and the generation of memory NK cells during MCMV infection (27). Up to now the molecular network underlying CD57^{+} phenotypes are mostly characterized by FACS techniques and microarray analyses on the systemic level (15, 17, 18).

Mass spectrometry can identify and quantify proteins in a global and unbiased manner, and thereby certainly contribute to the elucidation of developmental processes and the acquisition of specialized functions. Proteomic studies on human NK cells are accomplished mainly at the level of NK cell lines, because of the scarcity of primary NK cell subsets. Cytotoxicity, but not development, was studied in NK-92 and YTS NK cells by 2D-PAGE and peptide sequencing approaches pending on activating signals (28–32). At least one proteome study investigates *ex vivo* expanded primary human NK cells, and focuses on the characterization of kinases, involved in NK cell activation (33). Attempts to unravel the basics of NK cell development in mice were successful (34) but not completely transferable to the human NK cell system because of a different set of surface receptors. Hence, several studies have contributed to our understanding of the role of surface receptors in different developmental stages, but studies targeting the regulation of intracellular proteins are still missing.

In this study we characterized distinct developmental stages of primary human NK cells by proteomics. To get better insight into the molecular mechanisms of the NK cell differentiation process we comparatively analyzed freshly isolated primary CD56^{bright}, CD56^{dim}, CD56^{dim}CD57^{-} and CD56^{dim}CD57^{+} NK cells by isobaric tags for relative and absolute quantification (iTRAQ)-based LC-MS/MS. We obtained relative quantitative data for more than 3400 proteins and observed a specific CD56^{+} NK cell core proteome. The obtained proteomic data strongly supports the current differentiation model of NK cells by highlighting strong distinctions between CD56^{bright} and CD56^{dim} NK cells and high similarity among CD57^{-} and CD57^{+} NK cells. In addition to a significant set of anticipated and well-known proteins involved in NK cell development and effector functions, we detected also 11 novel protein candidates so far undescribed in NK cells. The expression patterns of S100A4 (UniProt accession name S10A4) and S100A6 (UniProt accession name S10A6), both belong to the family of S100 calcium binding proteins and contain two EF-hand domains, correlated with the developmental stages of cytotoxic NK cell subsets. Both proteins were recruited into the NKIS, following NK cell activation.

EXPERIMENTAL PROCEDURES

Monoclonal Antibodies and Reagents—For fluorescence-activated cell sorting (FACS), anti-CD56 (clone AF12–7H3, mouse IgG1, Miltenyi Biotec, Auburn, CA), anti-CD3 (clone HIT3a, mouse IgG1 κ, BD Bioscience), and anti-CD57 (clone TB03, mouse IgM, Miltenyi Biotec) mouse monoclonal antibodies (mAbs) were used. The following reagents were used: sodium chloride, 4-(2-hydroxyethyl)-1-piperazineethanesulfonic acid (HEPES), and Triton X-100 (Sigma), Mini Complete Protease Inhibitor Mixture Tablets (Roche), Benzonase (Merck), Trypsin (Promega, Madison, WI) and the iTRAQ Reagent Multiplex Kit (Applied Biosystems). Organic solvents, such as ethanol, methanol, and acetonitrile (ACN), were obtained from J. T. Baker Inc. For colocalization studies: anti-Perforin (mouse, deltaG9, BD Pharmingen); anti-CD107a (mouse, H4A3, BD Pharmingen); anti-CD107a (rabbit, 24170, Abcam, Cambridge, MA); Myosin IIa (non-muscle, rabbit, Sigma Aldrich); S10A4 (directed against S100A4; mouse, NJ4F3, Abcam), and S10A6 (directed against S100A6; mouse, CACY-100, GeneTex) were used.

Human NK Cells—This study was conducted in accordance with the rules of the Regional Ethics Committee of Lower Saxony, Germany and the declaration of Helsinki. Buffy coats from blood donations of healthy human volunteers who provided informed consent were obtained from the Institute for Clinical Transfusion Medicine, Klinikum Braunschweig, Germany. Blood donors' health is rigorously checked before being admitted for blood donation. This process included a national standardized questionnaire with health questions, an interview with a medical doctor and standardized laboratory tests for a) infections HIV1/2, HBV, HCV, Syphilis (serology and/or nucleic acid testing) and b) hematological cell counts.

Buffy Coats were produced from whole blood donations on day 1 by using the Top & Bottom Extraction Bag System (Polymed Medical Devices™, Triple Blood Bag System, No. 7300; containing CPDA-1. Peripheral blood mononuclear cells (PBMCs) were isolated from these buffy coat products by Biocoll density gradient centrifugation (Biochrome AG) on day 2. PBMCs were cultured overnight in RPMI 1640 medium (GIBCO) supplemented with 10% fetal bovine serum (FBS) gold (PAA Laboratories, Etobicoke, ON, Canada), 2 mM L-glutamine, 50 units/ml penicillin and 50 μg/ml streptomycin (all Invitrogen) at 37 °C in a humide 7.5% CO_2 atmosphere.

FACS Sorting—PBMCs were incubated with fluorochrome-conjugated anti-CD3, anti-CD56, and anti-CD57 monoclonal antibodies (mAbs) for 15 min at 4 °C on day 3. CD3^{-}CD56^{dim} and CD3^{-}CD56^{bright} NK cells as well as CD3^{-}CD56^{dim}CD57^{+} and CD3^{-}CD56^{dim}CD57^{-} NK cells were isolated by FACS using a FACSAria II flow cytometer (BD Biosciences; Bionozzle size: 70 μm; system pressure: 70 PSI; flow rate 30,000 events/sec; laser: 561 nm with 50 mWatt for PE; 640 nm with 60 mWatt for APC; detection: APC 670/14, PE 585/15; 488 nm with 100 mW for FITC; detection with bandpass filters for PE 585/15, APC 670/15 and FITC 525/50). The purity and viability of the NK cell subsets were assessed by flow cytometry. In all experiments, the purity of the isolated NK cell sub-

sets (CD3$^-$CD56^{bright}/CD56^{dim}; CD3$^-$CD56^{dim}CD57$^+$/CD57$^-$) was higher than 96%.

Cell Lysis, Protein Digestion, and iTRAQ Modification of Peptides—CD3$^-$CD56^{dim}/CD3$^-$CD56^{bright} (CD56^{dim} *versus* CD56^{bright}) and CD56^{dim}CD57$^+$/CD56^{dim}CD57$^-$ (CD57$^+$ *versus* CD57$^-$) NK cells were each isolated from five individual human donors and mass spectrometry data were obtained and processed for each of the 10 donors individually. At a minimum, 0.9×10^6 NK cells were used for each MS experiment. NK cells were lysed in ice-cold lysis buffer (50 mM HEPES pH 7.5, 150 mM NaCl, protease inhibitor mixture supplemented with EDTA, 1% Triton-X100) on day 3. Protein concentrations were determined using a NanoDrop spectrophotometer (ND-1000, Peqlab, Biotechnology GmbH, Erlangen). Proteins were extracted from lysates by chloroform/methanol precipitation as described previously (35), and redissolved in dissolution buffer (50 mM TEAB). Equal amounts of protein from each NK cell subset was digested with sequencing grade modified trypsin from Promega, as recommended in a ratio of 1:50 at 37 °C on day 3 overnight. Subsequently, digestion was completed by adding a further 1 μg of trypsin for 2 h to each sample. Labeling of tryptic peptides with isobaric iTRAQ reagents was performed on day 4, according to the manufacturer's guidelines (Applied Biosystems, Foster City, CA). Peptides derived from CD56^{dim} NK cells were labeled with iTRAQ reagent 117, those derived from CD56^{bright} NK cells were labeled with iTRAQ reagent 115 Da. For quantitative MS analyses of peptides from CD3$^-$CD56^{dim}CD57$^+$ (CD57$^+$) NK cells, iTRAQ label 114 was used, and iTRAQ 116 for CD3$^-$CD56^{dim}CD57$^-$ (CD57$^-$) NK cell peptides (supplemental Table S1; Supplement). Peptides of two different NK cell subsets (CD56^{bright} and CD56^{dim} or CD57$^-$ and CD57$^+$ NK cells) were combined (1:1 ratio), vacuum dried, dissolved in 0.2% trifluoroacetic acid and desalted on self-packed LiChroprep RP-18 (Merck) SPE columns.

Strong Cation Exchange Chromatography (SCX)—The combined iTRAQ-labeled peptide samples were further subfractionated by strong cation exchange chromatography (SCX) on day 4 to support representative and comprehensive protein identification by LC-MS/MS. Peptides were dissolved in SCX buffer (0.065% formic acid, 25% ACN) and fractionated on a Mono SPC1.6/5 column connected to an Ettan micro-LC system (both GE Healthcare), and separated at a flow rate of 150 μl/min for 30 min with a linear gradient from 0% to 35% SCX buffer supplemented with 0.5 M potassium chloride. Fractions were collected by a microfraction collector, every minute (SunCollect). Peptide elution was monitored by an UV detector at 214 nm. Peptide-containing fractions were vacuum-dried, desalted by RP-C_{18} chromatography ZipTip pipette tips (Millipore) and analyzed separately by LC-MS/MS.

LC-MS/MS Measurement and Protein Identification—LC-MS/MS analyses were performed with an UltiMate 3000 RSLCnano LC system (Thermo Scientific) connected to an LTQ Orbitrap Velos Fourier transform mass spectrometer (Thermo Scientific). Peptides were applied to a C_{18} precolumn (3-μm, Acclaim, 75 μm $\times$ 20 mm, Dionex) and washed with 0.1% TFA for 3 min at a flow rate of 6 μl/min. Subsequently, peptides were separated on a C_{18} analytical column (3-μm, Acclaim PepMap RSLC, 75 μm $\times$ 25 cm, Dionex) at 350 μl/min *via* a linear 120-min 3.7–31.3% B gradient with UPLC solvent A (0.1% formic acid in water) and UPLC solvent B (0.1% formic acid in 80% ACN). The LC system was operated with Chromeleon Software (version 6.8, Dionex). The effluent from the column was electrosprayed (Pico Tip Emitter Needles, New Objectives) into the mass spectrometer. The mass spectrometer was controlled by Xcalibur software (version 2.1, Thermo Scientific) and operated in the data-dependent mode allowing the automatic selection of doubly and triply charged peptides and their subsequent fragmentation. Peptide fragmentation was carried out using High Collision Dissociation (HCD) settings, with Collision Energy (CE) 44 optimized for iTRAQ-labeled peptides. MS/MS raw data from all SCX fractions, corresponding to one experiment, were visualized by Xcalibur software (.raw-file) and merged for Mascot Daemon-aided searches (Mascot version V2.3.02, Matrix Science) against UniProtKB/Swiss-Prot protein database (release 2011_03; with 525,997 entries; taxonomy: *Homo sapiens* with 20,226 entries). The following search parameters were used: enzyme, trypsin; maximum missed cleavages, 1; fixed modifications, iTRAQ^{TM} 4-plex (K), iTRAQ^{TM} (N terminus), Methylthio (C); variable modifications, oxidation (M); peptide ion mass tolerance, 10 ppm; MS/MS tolerance, 0,2 Da. Mascot result files (.dat files) were uploaded into the software Scaffold (Version Scaffold_3_00_01, Proteome Software Inc.), which was used for inspection of MS/MS data-based identification of peptides/proteins, to support protein quantifications and to prepare statistical validation and comparison of donor specific data sets, respectively. Only proteins with a minimal protein identification probability of 99% and identified by at least two unique peptides showing a minimal peptide identification probability of 95% and a Mascot (peptide) Score of at least 30 were accepted in this survey. Mascot-aided decoy searches were performed against the randomized Uniprot/Swiss-Prot protein database Mascot version V2.3.02, Matrix Science) against UniProtKB/Swiss-Prot protein database (release 2011_03; with 525,997 entries; taxonomy: *Homo sapiens* with 20,226 entries) and protein false discovery rates (FDRs) were calculated by Scaffold on the basis of FDR = FP (false positive)/(FP + TP (true positives)). On average we determined FDRs always lower than 0.9% (with significance level 0.05 in Scaffold). All MS-data associated with this manuscript are published in the PROteomics IDEntification Database (PRIDE) (www.ebi.ac.uk/pride/).

Protein Quantification—The Scaffold software (Version Scaffold_3_00_01, Proteome Software Inc.) was used for relative quantification of protein expression in NK cell subsets. Mascot result files (.dat files) were uploaded into Scaffold and all identified proteins as defined by the criteria described above were considered for quantitative data analyses. For quantification, only unique peptides were used. Scaffold provided normalized $\log_2$-regulation factors (RFs), basing on the iTRAQ-label intensity of individual peptides, respectively. Log_2 regulation factors represent the relative abundance of a protein in CD56^{dim} compared with CD56^{bright} or CD57$^+$ compared with CD57$^-$ NK cells (RF = CD56^{dim}/CD56^{bright}; CD57$^+$/CD57$^-$). Regulation factors calculated by Scaffold were exported to Excel (Microsoft Office 2007) and statistically analyzed.

Statistical Data Analysis—The aim of the statistical evaluation was to distinguish random fluctuations of protein regulation factors (RF) or potential donor variations from statistically significant and conserved regulations within the NK cell data sets. To identify significant protein regulations the variation of the regulation factors was statistically estimated. In our statistical model we assume that the $\log_2$-regulation factors (RF) of each protein follow a normal distribution ($5 \times \log_2$ RFs per protein because of five analyzed donors per NK cell subset comparison) with different expected values, but with the same standard deviation σ_0. It is necessary to estimate σ_0 to distinguish significant (donor-dependent) deviations from no regulation. The limited number of replicates ($n = 5$ donors in each of both comparative NK subset analyses) required an estimation of the standard deviation by taking RFs of all proteins into account. In our model we used the mean of the MADs (Median Absolute Deviation from the median) of all proteins as an estimator for the standard deviation of a normal distribution (with a correction for small sample sizes). The MAD was corrected by the factor of 1.4826 (determined by Monte Carlo simulation) according to the number of $k = 5$ data sets (donors) to obtain an unbiased and robust estimator for the standard deviation σ_0. In this way we obtain many estimates for the MAD with a large variance. But averaging this larger number of not very reliable estimates leads to a reliable estimate of the MAD.

Based on the previous estimation we are able to construct a hypothesis test for the identification of significantly regulated proteins. Thereby, the hypothesis of the test encompasses that a protein is considered to be significantly regulated if its mean regulation deviates significantly from 0. The function Φ represents the cumulative distribution function of the standard normal distribution. As previously shown, we propose a strict test (36), where α is the significance level of the test (here $\alpha = 5\%$; before FDR correction) and where the absolute value of the $\log_2$-regulation exceeds a given threshold c_α in at least m ($m = 3, 4, 5$) out of the $k = 5$ replicates. n_m is the number of proteins that have been measured in at least m replicates. We used this value for the FDR correction, because we cannot apply the test to proteins that have been measured in less than m replicates. Taken all the parameters together we obtained the value for the threshold as follows:

$$c_\alpha = \sigma_0 \cdot \Phi^{-1}\left(1 - \left(\frac{\alpha}{2 \cdot n_m \cdot \binom{k}{m}}\right)^{\frac{1}{m}}\right)$$

These thresholds (for $m = 5$, $m = 4$, and $m = 3$ donors) were used to define a set of significantly and donor-independently regulated proteins (36 proteins).

Microscopy of fixed NK Cells—NK cells were freshly isolated from PBMCs of healthy donors by negative selection using the NK cell Isolation Kit (Miltenyi Biotec). Target cells (K562- leukemia cells) were allowed to settle overnight on poly-L-lysine coated coverslips (Sigma Aldrich). Pure NK cells (≥ 96%), were added at a ratio of 1:1 and incubated for 5, 10, 15, 20, and 30 min, at 37 °C and 7.5% CO_2. Cells were fixed for 20 min with 2% paraformaldehyde (Sigma) in sterile PBS, permeabilized for 3 min in 0.5% Saponin (Sigma) in PBS and 1h blocked with 1% BSA in PBS, supplemented with 0.05% Tween-20 (Roth). Cells were stained (3) with anti-Perforin, anti-CD107a, anti-Myosin IIa, anti-S100A4, and anti-S100A6 mabs. Secondary antibody staining was performed with goat anti-mouse IgG, conjugated with Alexa 594 and goat anti-rabbit IgG, conjugated with Alexa 488) in 1:400 dilution supplemented with DAPI (1:1000). Imaging was performed on an Axiovert 135 microscope with HBO lamp and CCD camera. Images were analyzed by MetaMorph software, version 7.5.3.0 (Analytical Technologies). Five independent experiments were performed using pure NK cells and 20–30 images were acquired per coverslip in one experiment. Image analysis was performed with ImageJ (version 1.44p).

RESULTS

The Proteome of Primary Human CD56^{+} NK Cells—Comparative proteome studies of two distinct developmental steps, from CD56^{bright} to CD56^{dim} and from CD57^{-} to CD57^{+}, each from five healthy human blood donors were performed.

Peripheral blood mononuclear cells (PBMCs) were freshly isolated from buffy coats of clinically approved healthy blood donors. These PBMCs were separated to generate the different developmental stages of primary human CD56^{+} NK cells. The used gating strategy for distinct CD56^{+} NK cell subsets is depicted in Fig. 1*A*. PBMCs were gated on forward scatter area (FSC) *versus* side scatter area (SSC), which revealed the lymphocyte population. These were further gated on FSC area *versus* FSC height and SSC area *versus* SSC height to exclude doublets and aggregates (not shown). CD3^{-}CD56^{+} NK cells were gated on CD56^{dim} and CD56^{bright} subsets. The

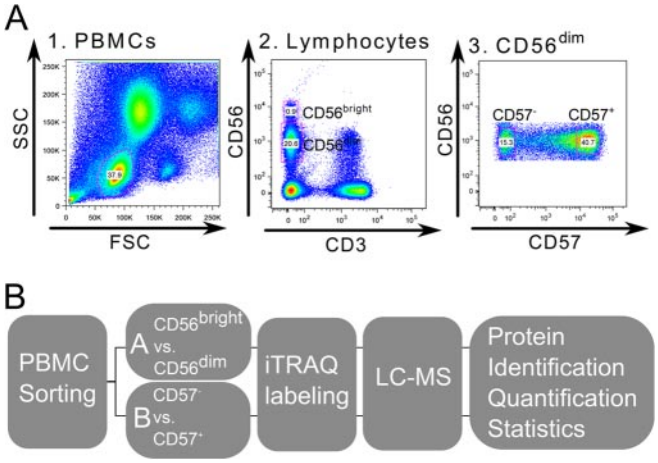

FIG. 1. **Isolation of distinct NK cell subsets and MS workflow.** *A*, Sorting procedure for NK cell subset isolation. Dot plot A1 depicts the PBMC population with gate on lymphocytes (blue). Gating on CD3^{-}CD56^{+} NK cells, with separate gates on CD56^{dim} and CD56^{bright} NK cells within the lymphocyte population is depicted in dot plot 2. Further discrimination of the CD56^{dim} NK cell population into CD57^{+} and CD57^{-} NK cell subsets is shown in dot plot 3. *B*, Experimental design of MS-based proteomic analysis of NK cell subsets. NK cell subsets were sorted from healthy human blood donor PBMCs to produce specific CD56^{pos} NK cell subsets. Isolated NK cells were prepared for MS analysis and differentially labeled with iTRAQ for further quantification. Labeled peptides were sequenced by nanoLC-MS/MS. Database searches supported protein identification and comparing iTRAQ reporter intensities revealed protein regulation factors. Statistical evaluation was performed on the generated datasets for quality control and to filter out conserved donor-independent protein regulations.

challenge here was to overcome the scarcity of CD56^{bright} NK cells, which account for only 5–10% of all NK cells. Therefore, 6×10^8 PBMCs were sorted for CD56^{+} NK cell subsets to obtain about 1×10^6 CD56^{bright} NK cells from each donor, sufficient material to study the first developmental step from CD56^{bright} to CD56^{dim}. Similarly, CD56^{dim} NK cells from further five healthy human blood donors (D6-D10; supplemental Table S1; supplemental Table S2) were isolated separately and sub-divided into CD57^{-} and CD57^{+} NK cell subsets to study the second developmental step.

CD56^{bright} NK cells were used to normalize (1) the cell numbers of subsets analyzed by proteomics and (2) the obtained protein regulatory data. Proteins were extracted directly from the freshly sorted primary NK cell subsets and digested with trypsin (Fig. 1*B*). Peptides originating from the distinct subsets were then labeled differentially by iTRAQ, combined and further subfractionated by strong cation exchange chromatography (SCX) to reduce ion suppression effects and to improve protein sequence coverage. Fifteen SCX fractions were analyzed for each donor by peptide sequencing (LC-MS/MS). In total, 415,203 fragmentation experiments of peptide ions were performed and searched against human entries of the UniProt Database. Considering result tables from all subsets revealed the expression of 3412 pro-

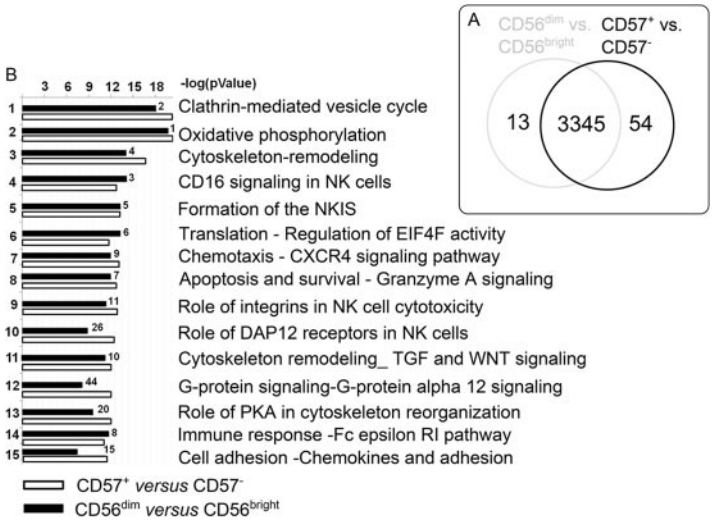

FIG. 2. **GeneGo™-based signaling pathway annotations of proteins identified in CD56^{+} NK cell subsets.** *A*, The Venn diagram depicts the numbers of identified proteins in CD56^{+} NK cells subsets. 3345 common proteins were identified in CD56$^{dim/bright}$ and CD57$^{+/-}$ NK cells. 13 proteins were unique in CD56$^{dim/bright}$ NK cells and 54 in CD57$^{+/-}$ NK cells. *B*, Data sets (all proteins, $n = 5$, median) were loaded into GeneGo™. This program assigns proteins to certain pathways by computing a statistical relevance value (negative log *p* value). The negative log *p* value depicts the ratio of proteins identified in this study and proteins known to be present within this pathway. Hierarchical order was defined by CD57^{-} NK cell subsets. Numbers depict the order within the CD56$^{bright/dim}$ GeneGo™ analysis.

teins in CD56^{+} primary NK cells. 3345 of those proteins were identified commonly in both comparative proteome approaches (Fig. 2*A*). Only 13 proteins were exclusively detected in the CD56$^{dim/bright}$ subsets and 54 in CD57$^{+/-}$ NK cell subsets (supplemental Table S3). Among these uniquely identified proteins, several signaling components, like UB2Q2 (Ubiquitin-conjugating enzyme E2 Q2; CD56$^{dim/bright}$), PTN9 (Tyrosine-protein phosphatase non-receptor type 9; CD57$^{+/-}$), P52K (52 kDa repressor of the inhibitor of the protein kinase; CD57$^{+/-}$), SLAP2 (Src-like-adapter 2; CD57$^{+/-}$), RN167 (E3 ubiquitin-protein ligase RNF167; CD57$^{+/-}$), CPPED (Calcineurin-like phosphoesterase domain-containing protein 1; CD57$^{+/-}$), and the C-X-C chemokine receptor type 2 CXCR2 (CD57$^{+/-}$) were detected. These proteins may possibly represent novel markers for the corresponding NK cell subsets, but a multiplicity was identified only in one donor (8 of 13 proteins in CD56$^{dim/bright}$ and 37 of 54 proteins in CD57$^{+/-}$ NK cell subsets, whereas four proteins showed RFs above the statistical thresholds, namely GTPB6 (Putative GTP-binding protein 6; CD56$^{dim/bright}$; $Log_2RF = -0.8$); ZN574 (Zinc finger protein 574; CD57$^{+/-}$; $Log^2RF = 0.7$); CLN5 (Ceroid-lipofuscinosis neuronal protein 5; CD57$^{+/-}$; $Log^2RF = 0.8$), and AMPN (Aminopeptidase N; CD57$^{+/-}$; $Log^2RF = 0.8$). All uniquely identified proteins are highlighted with an * in supplemental Tables S4 and S5). This minor difference regarding the number of proteins identified by our two-dimensional proteome strategy indicates that NK cell development does not depend on the presence but on the regulation of certain proteins. By evaluating individual donors, the comparison of CD56^{dim} *versus* CD56^{bright} NK cell subsets revealed 2941 common proteins, whereof 40% (1162) could be detected in all investigated donors. Corresponding numbers for the MS analyses of CD57^{+} *versus* CD57^{-} NK cells were 3224 and 1427 (44%) (supplemental Fig. S1). The 2941 identified proteins of the CD56^{dim}*versus* CD56^{bright} MS analysis are listed in supplemental Table S4 (supplemental excel file: CD56dimversusCD56bright.xls) and the detected proteins of the CD57^{+} *versus* CD57^{-} NK cell subset analysis (3224) are summarized in supplemental Table S5 (Supplemental excel file: CD57+versusCD57-.xls), including their Mascot Protein Scores, number of unique peptides, log_2 regulation factors and protein coverage for each individual donor investigation and as median value, including the five investigated donors.

All identified proteins were analyzed using GeneGo™, a tool which gives an overview about preferentially covered pathways. This bioinformatics analysis gave directly insight into the functionality of the investigated CD56^{+} NK cell proteomes and revealed predominant expression of two main biological processes: cytoskeleton re-arrangements and immune response pathways. Thereby, we observed striking similarities in pathway coverage between CD56$^{dim/bright}$ compared with CD57$^{+/-}$ NK cells, as indicated before (Fig. 2*A*). Also numerous NK cell signaling pathways were found highly represented by the identified proteins, *i.e.* CD16 signaling (identified proteins covered 50% of the entire pathway); formation of the immunological synapse (56%) and Granzyme A signaling (86%) (Fig. 2*B*). Hence, the GeneGo™ analysis confirmed a functionally consistent protein set in CD56^{+} NK cells subsets and underlines the presence of a putative core proteome.

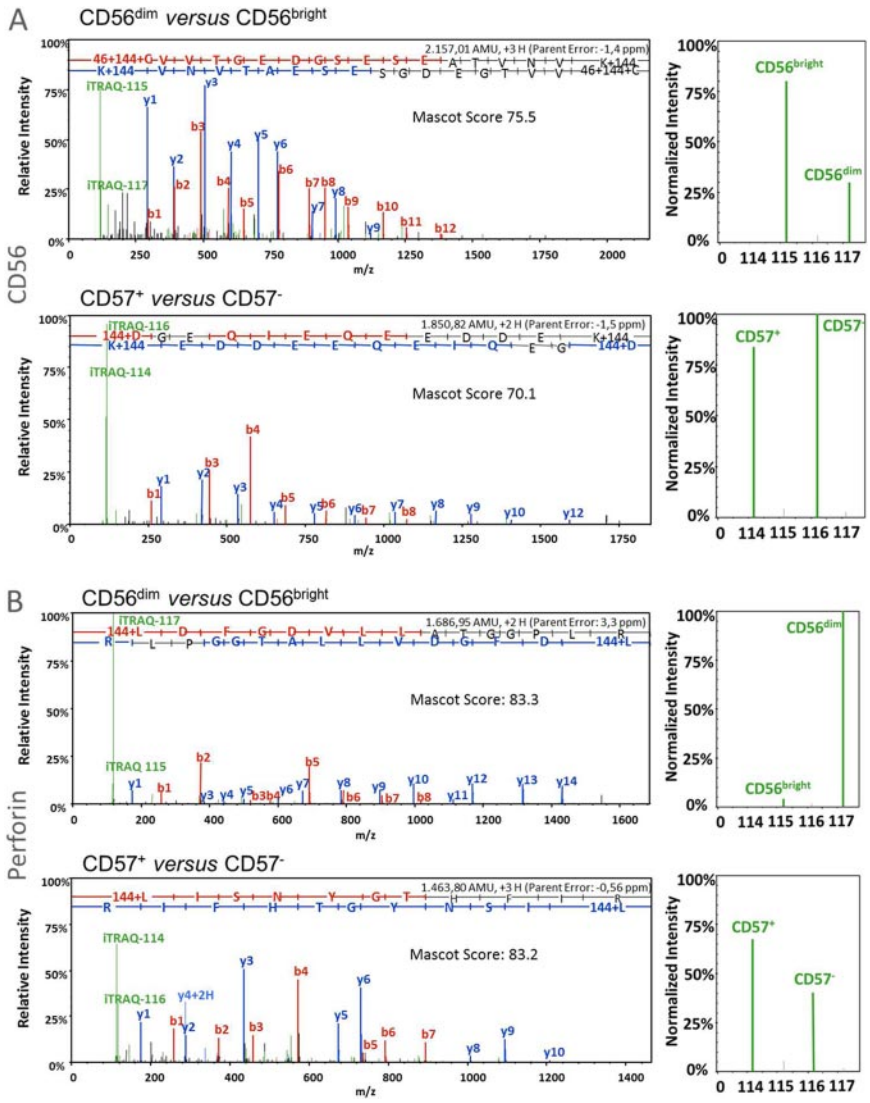

FIG. 3. **MS/MS spectra of peptides with corresponding iTRAQ^{TM} reporter intensities identified in CD56^{+} NK cell subsets.** Sorted NK cells were lysed, and trypsin-digested peptides were tagged with iTRAQ-label 115 (for CD56^{bright} NK cell subset) and 117 (for CD56^{dim} NK cell subset), or with 114 (for CD57^{+} NK cell subset) and 116 (for CD57^{-} NK cell subset). Subset peptides (CD56^{dim}*versus* CD56^{bright}, CD57^{+}*versus* CD57^{-}) were combined in 1:1 ratio and sequenced via nanoLC-MS/MS. Peptide fragmentation detected b (red)- and y (blue)-ions. Peptide sequences were derived from these ions through defined amino acid masses. Through Mascot-based database searches in UniProt/Swiss-Prot, peptide sequences were assigned to the proteins CD56 (*A*) and Perforin (*B*). Quality of this assignment depends on high peptide Mascot Scores. iTRAQ reporters occur in low mass regions of the spectrum (green). By comparing normalized reporter intensities (115-ref against 117 and 114 against 116-ref), peptide abundances were quantified and $\log_2$-regulation factors (RFs) were generated. The RFs of all identified peptides of one protein represent the corresponding protein regulation factor.

Evaluating NK Cell Specific Protein Expression—Donor and subset specific peptide samples were labeled differentially with iTRAQ reagents for relative quantification in addition to peptide sequencing. Thus, each individual MS fragment ion spectrum provides quantitative information in parallel to the identified peptide sequence. The ratios of iTRAQ reporter intensities were used to determine the relative protein abundances in the different CD56^{+} NK cell subsets-1D-LC-MS/MS experiments were performed with 1% of each sample to confirm the completeness of peptide labeling. Next, manual inspection of the quantitative data using Scaffold uncovered a set of well-described NK cell-specific proteins. For example, expression of CD56 (NCAM1) and Perforin (PERF) is fully in accordance with the literature: CD56 expression declines from CD56^{bright} to CD56^{dim} NK cells, whereas Perforin abundance increases simultaneously (Figs. 3*A* and 3*B*) (37). Furthermore, a stable CD56 expression in CD57^{+} and CD57^{-} NK cells was recently described (15). MS data of this study indeed confirm non-regulated CD56 expression profiles and in parallel revealed a slight increase in Perforin abundance in CD57^{+} NK cells. Thus, abundances of well-described NK cell proteins are in perfect accordance with the literature

(supplemental Table S6) (15–17, 37). Regarding to NK cell differentiation the level of cytotoxicity related proteins, like Perforin, multiple Granzymes and LAMP1/3 increases from CD56^{bright} to CD56^{dim} NK cells and induction of Perforin, as well as KIR expression coincides with CD57 appearance (15, 37).

Characterizing Donor-specific Variations—Although the blood donor volunteers were clinically approved to be healthy, we paid particular attention to determine potential individual variations.

A global inspection of regulatory data from each donor was performed by box plot analysis. Protein regulation factors in assessed donors were symmetric and normally distributed within the box plots, which indicates data robustness and only minor donor variations in both separate comparative analyses of CD56$^{dim/bright}$ and CD57$^{+/-}$ NK cell data. A wide regulation range from +3.8 to −4.0 (log_2RF = log_2 regulation factor) was detected in CD56$^{dim/bright}$ NK cells and only minor regulation differences in CD57$^{+/-}$ NK cells (+2.3 to −2.3; Fig. 4*A*, right hand panel).

Next, regulatory information were sorted at the protein level and inspected by heat maps (Fig. 4*B*). Generally, the expression profiles indicate a remarkable ratio of proteins similarly regulated in each set of five donor samples. As already indicated by the box plot analyses, a higher total number and more pronounced protein regulations were observed in CD56$^{dim/bright}$ NK cells compared with CD57$^{+/-}$ NK cells. Only slight donor variations could be detected for donor 3 of the CD56^{dim} and CD56^{bright} NK cell subsets and donor 8 of the CD57$^{+/-}$ NK cell subsets. Hence, the heat map analyses generally confirmed reproducible quantification and highly conserved protein regulation signatures within both sets of donors. Individual variations are limited and thus likely not compromise the definition of conserved regulated proteins. However, their identification might be of interest as clinical markers. Thus, we characterized strongly deviating proteins, which occur donor-dependently, through MAD analysis. Proteins with a MAD higher than 0.3, were considered to show donor-dependent protein regulations. The vast majority of proteins exhibited remarkable consistent protein. However, 13 proteins were found with MAD values higher than 0.3 and therewith donor-dependent protein deviations. Ten of those cases were detected in CD56$^{bright/dim}$ and three in CD57$^{+/-}$ NK cells. The 13 candidates include GRAH (Granzyme H) and GNLY (Granulysin), which were already previously described to be donor-dependently regulated in human primary lymphocytes (38, 39) (supplemental Fig. S2). Another strongly deviating candidate is CD44, whose regulation occurs infection-dependently in mice and steers human postnatal thymocyte development (40, 41). CD63 (Granulophysin) is well characterized in NK cells and was shown to be differentially regulated in decidual human primary NK cell subsets (42). CATW (Cathepsin W) is exclusively expressed in CD8^{+} T cells and NK cells. This protein may mediate cytolytic activity, but is not essentially involved in cytotoxicity (43). Unfortunately, donor-dependent expression patterns of CD44, CD63, CATW and the other proteins with high MAD values have not been accessed to this date in primary human NK cells.

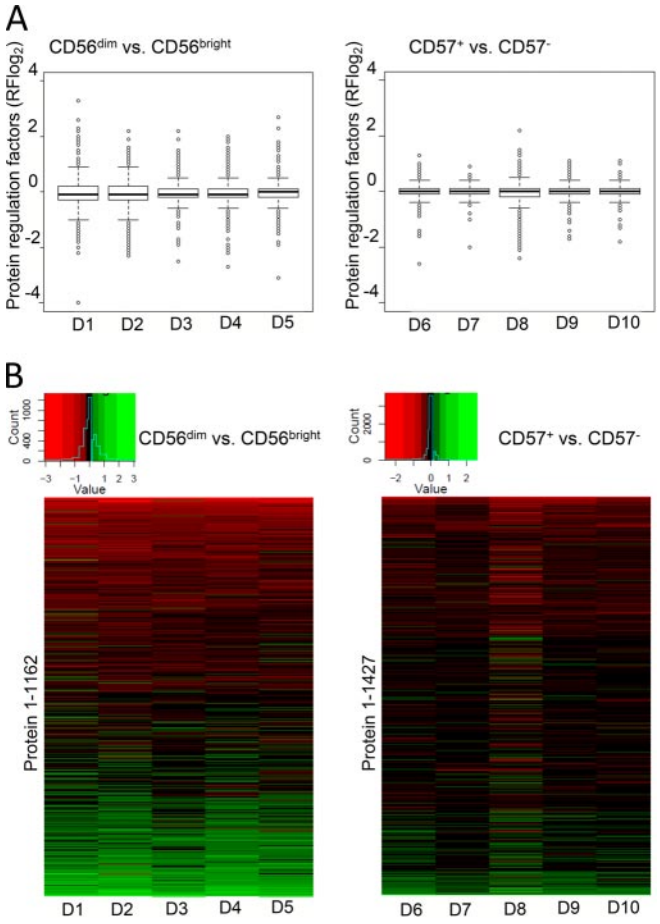

FIG. 4. **Statistical evaluation of CD56^{+} NK cell subset data.** *A*, Box plots of protein regulation factors in CD56$^{dim/bright}$ and CD57$^{+/-}$ NK cell subsets. The box of each graph displays 50% of all determined protein regulation factors, the box height depicts their spreading and the black line within the boxes indicates the median. The restricting lines (high and low Whisker) display 1.5 × height of the box. All protein regulation factors above or beneath the Whiskers are categorized as strongly regulated and are shown as light dots. The symmetric distribution of protein regulations in all assessed donors with slight fluctuations is visible. Regulation ranges differ strongly within CD56$^{dim/bright}$ (between +3.8 and −4) and only slightly within CD57$^{+/-}$ NK cells (between +2.3 and −2.3), corresponding to their individual stage of differentiation. *B*, Heat maps of log_2-protein regulation factors determined by iTRAQ-based LC-MS/MS from primary human CD56^{+} NK cell subsets. Heat maps were generated by loading NK cell subset-specific lists of proteins, identified in all five assessed human blood donors by iTRAQ-based LC-MS/MS, into the statistical program R (1162 in CD56$^{dim/bright}$ and 1427 within CD57$^{+/-}$ NK cells). Colored boxes in one row depict the regulation of one protein in five individual blood donors. One row depicts protein regulations in one blood donor. The histogram above displays the distribution of protein regulation factors and the corresponding color code.

In conclusion, donor dependent variations were observed to a minor degree (13 proteins among 3412) in this study.

Regulations of well-described NK-specific proteins serve without exception as proof-of-concept data. A broader dynamic range of regulations coinciding with the step from CD56^{bright} to CD56^{dim}, compared with the subsequent step from CD57$^-$ to CD57$^+$, confirmed the recently suggested differentiation model. On the other hand, regulations observed for proteins so far not described in this context likely contribute to the biology of distinct NK cell subsets, including NK cell effector functions, status of differentiation and responsiveness.

Subset-specific Protein Regulation in CD56$^+$ NK Cell Development—After investigating donor variation, particular attention was paid to the detection of the most significant and subset-specific protein regulations. Therefore, a statistical model was developed to detect the most pronounced and conserved protein regulations (36). Standard deviations were calculated based on the assumption that $\log_2$-regulation factors of each protein follow a normal distribution, taking the limited number of 5 donors into account. The 3412 identified proteins were used to estimate the standard deviation and this served as a base to determine statistical significance thresholds depending on the number of donors. Notably, the thresholds considering only 3 donors (0.83 for CD56$^{dim/bright}$ and 0.51 for CD57$^{+/-}$ NK cells) did not vary significantly from thresholds calculated for four or five donors ($\log_2RF_{CD56dim/bright}$: 0.809 and 0.745 and $\log_2RF_{CD57\pm}$: 0.503 and 0.467; see supplemental Table S8). Hence, the thresholds 0.83 for comparing CD56^{dim} *versus* CD56^{bright} NK cells and 0.51 for CD57$^+$ *versus* CD57$^-$ NK cells were applied to extract subset-specific protein regulations. Although the threshold for CD56$^{dim/bright}$ NK cell subsets was significantly higher than in CD57$^{+/-}$ NK cells, a list of 31 proteins was generated (Table I), instead of 5 proteins in CD57$^{+/-}$ NK cell subsets (Table II).

None of these 36 proteins belongs to the group of donor-dependently regulated candidates with MAD values over 0.3. Thus, the regulation of these 36 proteins can be directly related to the distinct developmental NK cell stages. They can be grouped into the following categories: (1) NK signaling; (2) cytoskeletal dynamics; (3) differentiation and (4) cytotoxicity. Top-regulated novel CD56$^+$ NK cell protein candidates (11 proteins; depicted in bold; with $-1.0<\log_2RF>1.0$, Fig. 5) are comparatively and subset-specifically summarized together with six key components of NK cell biology in FIGURE 5. Among those, the expression of the AK1C3 (Aldo-keto reductase family 1 member C3) protein was highest in CD56^{dim} NK cells together with Perforin and declined within the last step of differentiation into CD57$^+$ NK cells. Expression of NHRF1 (Na^+/H^+ exchange regulatory cofactor NHE-RF1), SH2K1 (SH3 domain-containing kinase-binding protein 1), EFHD2 (Swiprosin), ANXA2 (Annexin A2) and PTCA (Protein tyrosin phosphatase receptor type C-associated protein) increased during the first differentiation step from CD56^{bright} into CD56^{dim} NK cells and was stagnating during the last step from CD57$^-$ to CD57$^+$ NK cells.

However, we also detected proteins highly abundant in CD56^{bright} NK cells, with a decline in expression during all following differentiation steps (from CD56^{dim} to CD57$^-$ and finally to CD57$^+$ NK cells), *e.g.* FLNB (FilaminB), LMNA (PrelaminA/C), and COTL1 (Coactosin-like protein), which indicates a pivotal role especially in this early NK cell subset. In total three proteins showed continuous increase in expression during both differentiation steps, namely S100A4 (Calvasculin), S100A6 (Calcyclin), and LEG1 (Galectin-1). LEG1 was previously described in NK cells, but without NK cell subset-specific regulation. Of note, all three proteins were shown previously to be involved in the thymocyte differentiation process (52).

S100A4 and S100A6 are Recruited to the NKIS and Colocalize with Myosin IIa—NK-cell cytotoxicity depends on the formation of the F-actin-rich NKIS and the Myosin IIa (MYH9) mediated transport of Perforin-containing lytic granules to the NKIS (3–5). In this study, we detected MYH9 expression highest in mature CD56^{dim} ($\log_2RF = 0.7$), but reduced in terminally maturated CD57$^+$ NK cells ($\log_2RF = 0.1$), confirming its relevance for cytotoxic NK effector functions. Like MYH9, other subset-specific proteins exhibit a similar expression profile, *e.g.* S100A4 and S100A6. Notably, MYH9 was previously shown to interact with S100A4 in murine fibroblasts (NIH3T3) and human endothelial cells (CSML-0 and −100) (44, 45). Therefore, both proteins (S100A4 and S100A6) were selected for subcellular localization studies that were performed using cytotoxic CD56^{dim} (with high Perforin expression levels) NK cells to analyze S100A4 and S100A6 contribution to the immunological synapse of NK cells. NK activation was performed by coincubation with their natural targets - K562 cells that we conducted in a time-resolved manner for 5, 10, 15, 20, and 30 min. The induced formation of the NKIS was documented by fluorescence microscopy. Staining for Perforin together with CD107a (46) and MYH9 (3) allowed following the dynamics of formation and recruitment of lytic granules to the interphase between NK and target cell. All three proteins localized time-dependently into the NKIS, thus favoring this generally Fig. 6 and Fig. 7, left panel). Intensity of colocalization was determined with the help of 3D density surface plots, generated by ImageJ.

Microscopic investigation revealed time-resolved colocalization events of the here characterized NK cell proteins S100A4 and S100A6 together with MYH9. First colocalization between S100A4 and MYH9 was observed already after 5 min, formation of complete complexes after 10 min that peaked after 15 min, when specific recruitment and intense accumulation of this complex to the NKIS was observed (Fig. 6). Instead, peak accumulation of the S100A6 and MYH9 complex occurred already after 10 min (Fig. 7). The disassembly of this complex then starts immediately after 15 min whereas the S100A4 and MYH9 interactions lasted longer and started to disintegrate after 20 min and were apparent for

TABLE I

Threshold-determined (+/− 0.83, n = 3) list of 31 significantly regulated proteins in CD56$^{dim/bright}$ NK cell subsets. Included are UniProt accession names and numbers, as well as protein names. The median Mascot Score = median (n = 5) value of the peptide Mascot Scores sum per protein, median log_2-RF = median of the log_2-protein regulation factors of 5 approached donors, MAD value of the log_2-regulation factors and Median Protein Coverage in [%]. Functions are transferred from UniProt and were integrated into the following categories: (1) NK signaling; (2) Cytoskeletal dynamics; (3) Differentiation, and (4) Cytotoxicity with corresponding references

UniProt acession name	UniProt accession number	Protein name	Median mascot score	Median log_2-RF	MAD	Median protein coverage [%]	Function	Category	Reference
AK1C3	P42330	Aldo-keto reductase family 1 member C3	286	1.9	0.3	14	Converts aldehydes and ketones into alcohols, involved in hormone system, marker for "normal NK cells"	1	Choi et al., 2004
PERF	P14222	Perforin-1	1145	1.9	0.1	24	Key role in cytolysis, forms large pores, facilitates the uptake of cytotoxic Granzymes	4	Thiery et al., 2011
PKHF1	Q96S99	Pleckstrin homology domain-containing family F member 1	129	1.5	0.2	7.9	May induce apoptosis through lysosomal-mitochondrial pathway, initiates permeabilization of lysosomal membrane, results in release of PDCD8	4	Chen et al., 2005
S10A6	P06703	Calcyclin	182	1.5	0.2	17	Calcium sensor, plays a role in reorganization of actin cytoskeleton/ motility	2	Nedjadi et al., 2009
GRAP2	O75791	GRB2-related adapter protein 2	138	1.4	0.25	7.45	Interacts with SLP-76 to regulate NF-AT activation, binds to tyrosine-phosphorylated shc.	1	Qiu et al., 1998
S10A4	P26447	Calvasculin	961	1.3	0.1	36	Involved in thymocyte differentiation together with S10A6 and Galactin 1 (LEG1), regulates MYH9 acticvity	3	Jeon et al., 2009
CAN2	P17655	Calpain-2 catalytic subunit	338	1	0.1	9.4	Involved in cytoskeletal remodeling and signal transduction, regulates lamellopodia dynamics	2	Potter et al., 1998 Franco et al., 2004
FCG3A	P08637	Low affinity immunoglobulin gamma Fc region receptor III-A	118	1	0.1	9.8	Receptor for Fc region of IgG, mediates antibody-dependent cellular cytotoxicity (ADCC) and other antibody-dependent responses, such as phagocytosis (CD16a)	1	de Haas et al., 1996
VINC	P18206	Vinculin	2273	1	0	31	F-actin-binding protein involved in cell-matrix adhesion and cell-cell adhesion, may also play important roles in cell morphology and locomotion	2	Le Clainche et al., 2010
ANXA4	P09525	Annexin A4	936	1	0.2	39	Calcium/phospholipid-binding protein which promotes membrane fusion and is involved in exocytosis and synaptic endocytosis, promotes vesicle aggregation	4	Kaetzel et al., 2011
PDLI2	Q96JY6	PDZ and LIM domain protein 2	166	1	0.1	15	Promotes cell attachment, necessary for migratory capacity of epithelial cells	2	Loughran et al., 2005
PHTNS	Q6NYC8	Phostensin	435	1	0.1	18	May target protein phosphatase 1 to F-actin cytoskeleton	2	Kao et al., 2007
FCERG	P30273	High affinity immunoglobulin epsilon receptor subunit gamma	201	1	0.1	33	High affinity receptor for the Fc region of immunoglobulins gamma, functions in innate and adaptive immune responses	1	van Vugt et al., 1996

TABLE I—*continued*

UniProt acession name	UniProt accession number	Protein name	Median mascot score	Median log_2-RF	MAD	Median protein coverage [%]	Function	Category	Reference
SYNE2	Q8WXH0	Nesprin-2	582	0.9	0.1	1.2	Forms a network between organelles and actin cytoskeleton, maintains nuclear organization and structural integrity	2	Zhang et al., 2001
NHRF1	O14745	Na(+)/H(+) exchange regulatory cofactor NHE-RF1	1498	0.9	0.3	33	Scaffold protein, connects plasma membrane proteins with members of the Ezrin/Moesin/Radixin family, link them to actin cytoskeleton, may enhance Wnt signaling	2	Yun et al., 1997
SH3K1	Q96B97	SH3 domain-containing kinase-binding protein 1	732	0.9	0.1	22	Adaptor in signal transduction pathways, regulates endocytosis and lysosomal degradation, regulation of cell adhesion, cellular stress response and cell morphology/ cytoskeletal organization, controls of cell shape and migration	1	Szymkiewicz et al., 2002
EFHD2	Q96C19	EF-hand domain-containing protein D2 (Swiprosin)	1643	0.9	0.1	45	Regulates BCR-induced apoptosis, expressed in CD8+ T cells, may be involved in cytotoxic mechanisms	4	Dütting et al., 2011 Vuadens et al., 2004
ANXA2	P07355	Annexin A2	2352	0.9	0.3	51	Calcium-regulated membrane-binding protein, coats the surface of enlargeosomes needed for their regulated exocytosis	4	Deora et al., 2004 Lorusso et al., 2006
PTCA	Q14761	Protein tyrosine phosphatase receptor type C-associated protein	166	0.9	0.1	20	CD45-associated protein, promotes T cell activation	1	Veilette et al., 1999
LKHA4	P09960	Leukotriene A-4 hydrolase	796	-0.9	0.1	22	Epoxide hydrolase, catalyzes the final step in the biosynthesis of the proinflammatory mediator leukotriene B4	1	Tholander et al., 2008
MCM3	P25205	DNA replication licensing factor MCM3	189	-0.95	0.05	5.35	DNA replication initiation and elongation in eukaryotic cells, required for DNA replication and cell proliferation	1	Lee et al., 2009
CD2	P06729	T-cell surface antigen CD2	192	-1	0.2	12	Interacts with lymphocyte function-associated antigen (LFA-3) and CD48/ BCM1 to mediate adhesion between T-cells and other cell types, implicated in triggering T-cells and NK cells	2	Sabry et al., 2011
FABP5	Q01469	Fatty acid-binding protein, epidermal	185	-1	0.3	19	High specificity for fatty acids, decreasing the chain length or introducing double bonds reduces affinity. May be involved in keratinocyte differentiation	3	Hagens et al., 1999

TABLE I—*continued*

UniProt acession name	UniProt accession number	Protein name	Median mascot score	Median log_2-RF	MAD	Median protein coverage [%]	Function	Category	Reference
CD44	P16070	CD44 antigen	677	-1.2	0.3	6.2	Receptor for hyaluronic acid (HA), mediates adhesion, plays important role in cell migration, involved in lymphocyte activation, recirculation and homing, and in hematopoiesis	2	Sague et al., 2004 Crosby et al., 2009
LMNA	P02545	Prelamin-A/C	939	-1.3	0.2	27	regulates telomere dynamics	3	Gonzalez-Suarez et al., 2009
A2MG	P01023	Alpha-2-macroglobulin	228	-1.3	0.25	1.2	Inhibit all four classes of proteinases contains specific cleavage sites for different proteinases	4	Lin et al., 2005
FLNB	O75369	Filamin-B	1223	-1.3	0	11	Anchors various transmembrane proteins to actin cytoskeleton, essential for crossing the lymphoid barrier to invade blood epithels	2	Kanters et al., 2008
NCAM1	P13591	Neural cell adhesion molecule 1	291	-1.4	0.3	7	Cell adhesion molecule involved in neuron-neuron adhesion, interacts with fibroblasts, involvement in differentiation suggested	3	Chan et al., 2007
GRAK	P49863	Granzyme K	384.5	-1.7	0.1	28.5	Cytotoxic molecule in CD56^{bright} NK cells, promotes T cell killing to shape adaptive immune responses	4	Jiang et al., 2011
HVCN1	Q96D96	Voltage-gated hydrogen channel 1	104	-1.8	0.1	7.7	Forms a proton-selective channel through which protons may pass in accordance with their electrochemical gradient	1	Ramsey et al., 2006
CAPG	P40121	Macrophage-capping protein	573	-1.9	0.2	20	Calcium-sensitive protein, blocks barbed ends of actin filaments, may play a role in regulating cytoplasmic and/or nuclear structures	2	Hubert et al., 2009
COTL1	Q14019	Coactosin-like protein	761	-2.2	0.3	35	Binds to F-actin in a calcium-independent manner, regulator of Leukotrine metabolism	1	Rakonjac et al., 2006

further 10 min until full disintegration and detachment of the NK cell from the target cell.

To summarize, complex formation of S100A6 and MYH9 occurred very quickly, but between S100A4 and MYH9 much more intense and over a longer period of time. Hence, the microscopic investigation on the NK cell subset specifically regulated proteins S100A4 and S100A6, revealed distinct localization of both proteins at the NKIS after NK cell activation, followed by intense colocalization together with MYH9.

DISCUSSION

Research on NK cell development has rapidly emerged during the past few years, starting with the introduction of the four-step NK cell differentiation model, leading to fully active CD56^{bright} cells (9), their conversion into CD56^{dim} cells (12, 13) and their final complementation into terminally differentiated CD56^{dim}CD57$^+$ NK cells (15,17,18).

NK cell subset analyses mostly relied on FACS-based approaches and microarray analyses to determine subset specific protein expression from *ex vivo* expanded primary NK cells (11, 15, 37). As a complementation of these approaches, mass spectrometry can provide an unbiased and systematic overview about protein expression and regulation in the distinct developmental stages. Here, we provide the first insight into the proteome of primary CD56$^+$ NK cells of distinct developmental stages isolated from healthy human blood donors. We investigated the proteomes of CD56^{bright} *versus* CD56^{dim} and CD57$^-$*versus* CD57$^+$ NK cell subsets. Quantitative data were determined for 3400 proteins and describe

TABLE II

Threshold-determined (+/− 0.51, n = 3) list of 5 significantly regulated proteins within the CD57$^{+/-}$ NK cell subsets. Included are UniProt accession names and numbers, as well as protein names. The median Mascot Score = median (n = 5) value of the peptide Mascot Scores sum per protein, median log$_2$-RF = median of the log$_2$-protein regulation factors of five approached donors, MAD value of the log$_2$-regulation factors, Median Protein Coverage in [%]. Functions are transferred from UniProt and were integrated into the following categories: (1) NK signaling; (2) Cytoskeletal dynamics; (3) Differentiation, and (4) Cytotoxicity with corresponding references

UniProt accession name	UniProt accesion number	Protein name	Median mascot score	Log$_2$-RF median	MAD	Median protein coverage [%]	Function	Category	Reference
GRAK	P49863	Granzyme K	242	-1.7	0.3	6	Cytotoxic molecule in CD56^{bright} NK cells, promotes T cell killing to shape adaptive immune responses	4	Jiang et al., 2011
F169A	Q9Y6X4	Protein FAM169A	153	0.6	0.1	3.3	Unknown	-	-
LEG1	P09382	Galectin-1	328	0.6	0.1	45	Regulates apoptosis, differentiation and proliferation	3	Molvarec et al., 2011
S10A4	P26447	Calvasculin	261	0.6	0.3	36	Involved in thymocyte differentiation together with S10A6 and Galactin 1 (LEG1), regulates MYH9 activity	3	Jeon et al., 2009
COTL1	Q14019	Coactosin-like protein	212	-1.6	0.2	11	Binds to F-actin in a calcium-independent manner, regulator of Leukotrine metabolism	1	Rakonjac et al., 2006

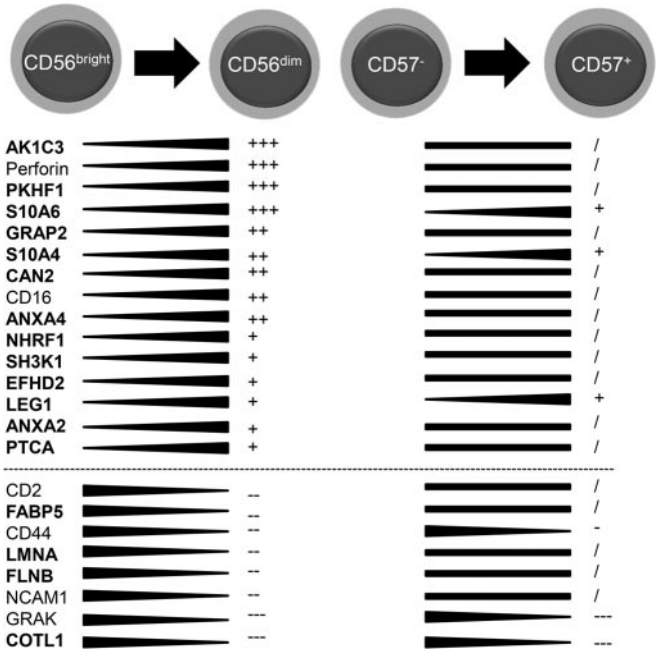

FIG. 5. **Changes in protein expression during distinct stages of NK cell differentiation.** Selected proteins are shown together with their corresponding regulation intensity in CD56$^{bright/dim}$ and in CD57$^{-/+}$ NK cells. Proteins with previously undescribed regulation in NK cells are shown in bold. Regulation intensity is depicted with the following symbols: +++ log$_2$RF over 1.5; ++ log$_2$RF over 1.0; + log$_2$RF over 0.5;/unregulated (in between −0.5 and 0.5); - less than −0.5; - less than −1.0; — less than −1.5.

already known as well as novel functional aspects of NK cell subsets. Notably, regulatory data of well-characterized NK cell proteins were in accordance with gene expression data from previous studies (16, 37).

CD56^{bright} cells characterize an immune regulatory NK cell subset able to release various pro-inflammatory cytokines for activating, modulating and recruitment of adaptive immune cells (11). CD56^{dim} NK cells also release cytokines, but their main biological function encompasses the detection of transformed and virus infected target cells, followed by target cell lysis (47). This cytotoxic capacity requires expression of cytolytic components, like Granzymes, Perforin, and Granulysin, as well as vesicle forming and transport related proteins (CD107a, Rab proteins, WASP), also involved in endocytosis. Our proteome approach covered a significant portion of known cytolytic and vesicle-forming components, which were consistently, detected less abundantly in CD56^{bright} NK cells but significantly higher amounts in CD56^{dim} cells that present the mature and prototypic cytotoxic NK subset.

Recently, it was reported that CD57 expression occurs independently of, but simultaneously with KIR acquisition and thus NK cell differentiation proceeds un-coupled, but in parallel to NK cell education. Our proteome results confirmed this observation, because KIR2DS2, KIR3DL2, and KIR3DL1 were solely detected regulated in the CD57^{+} NK cell subsets (supplemental Table S6). This study also provides evidence for the

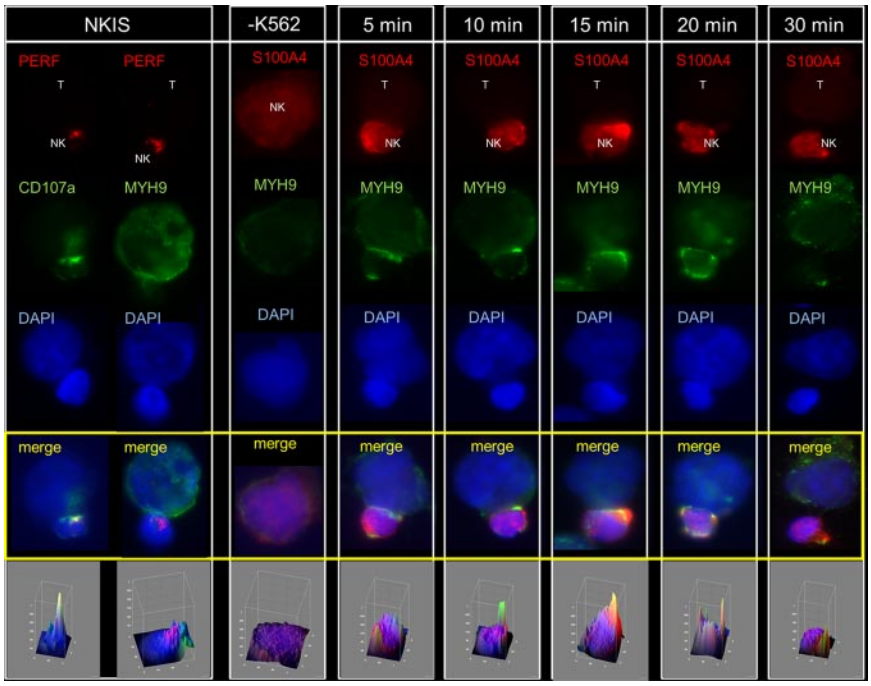

FIG. 6. **Time-resolved colocalization studies of S100A4 and MYH9 in activated NK cells.** NK cells were incubated and activated with K562 target cells ('T' for target cell and "NK" for NK cell) for 5, 10, 15, 20, and 30 min. First two rows show proof of concept colocalization events between Perforin (red) and CD107a (green), and between Perforin (red) and MYH9 (green). Time-resolved activation of NK cells and stain for S100A4 (red) and MYH9 (green) and DNA (DAPI, blue) with appropriate antibodies revealed remarkable time-dependent formation of colocalization events at the NKIS. Anti S100A4 was stained with goat anti-mouse IgG (Alexa 594) and anti-MYH9 (Myosin IIA) with goat anti-rabbit IgG (Alexa 488) supplemented with DAPI (1:1000). Imaging was performed on an inverted microscope (Axiovert 100TV; Carl Zeiss, Jena, Germany) microscope using standard epifluorescence illumination (light source HXP120, Zeiss) and 63×/NA1.4 or 100×/NA1.4 plan-apochromatic objectives. Imaging was performed at room temperature with immersion oil. Images were acquired with a back-illuminated, cooled charge-coupled-device camera (CoolSNAP HQ2, Photometrics, Tucson, AZ, USA) driven by Metamorph software (Version 7.5.3.0; Molecular Devices Corp., Downingtown, PA, USA). Five independent experiments were performed and 20–30 images were acquired per coverslip in each experiment. Image analysis was performed with ImageJ (version 1.44p).

specialization of terminally mature CD57$^+$ NK cells, because expression of KIRs and broad coverage of CD16 signaling-associated components (50% of the whole pathway) were determined only for this NK cell subset. It has been shown previously, that the intensity of NK cell cytotoxicity occurs donor-dependently (48, 49). Interestingly, donors of this study were clinically approved as healthy but statistical proteome analyses revealed slight but significant variations that might serve as markers to better understand these donor-variations. Although the majority of identified regulations (Table I and Table II) were found conserved and widely donor-independent, a limited number of protein regulation showed a MAD value higher than 0.3 (in summary 13 proteins). Among them we detected nine proteins with significant regulations, crossing the statistical threshold (supplemental Table S7). Four of them, GRAH (Granzyme H), CATW (Cathepsin W), and CD63 (LAMP-3), are well-characterized NK cell specific proteins involved in cytotoxicity and antigen processing, whereas CD44 is also known as marker for early T cell development in the thymus. The other three, protein kinase C (PACN1), SH2 domain containing protein 1A (SH21A) and MAP kinase 3 (MK03), are generally involved in NK cell signaling but were characterized as regulated in distinct developmental stages here for the first time. Unfortunately, the function of FETUA (Alpha-2HS glycoprotein) and CLIC3 (Chloride intracellular channel protein 3), showing most pronounced regulation, remain unknown in NK cells.

Particular attention was paid to determine statistically conserved NK subset-specific proteins. Thirty six proteins were detected by this approach and functionally categorized. LEG1 (Galectin-1), S100A4 (Calvasculin), and S100A6 (Calcyclin) occurred with pronounced increasing expression profiles both during the first and the second maturation step, indicating their general relevance in NK cell biology. LEG1 was described previously as significantly expressed and secreted by activated T_{reg} cells from mice and men (50, 51). Furthermore, it was shown that LEG1, S100A4 and S100A6 promote thymocyte differentiation (52). S100A4 and S100A6 belong to the calcium-binding family of S100 proteins and are generally involved in cell cycle progression and differentiation. For S100A4 a direct interaction with MYH9 was determined at the leading edge of migrating cells, which naturally contains a high calcium concentration (45). Because MYH9 is also known to play an important role by mediating the interaction

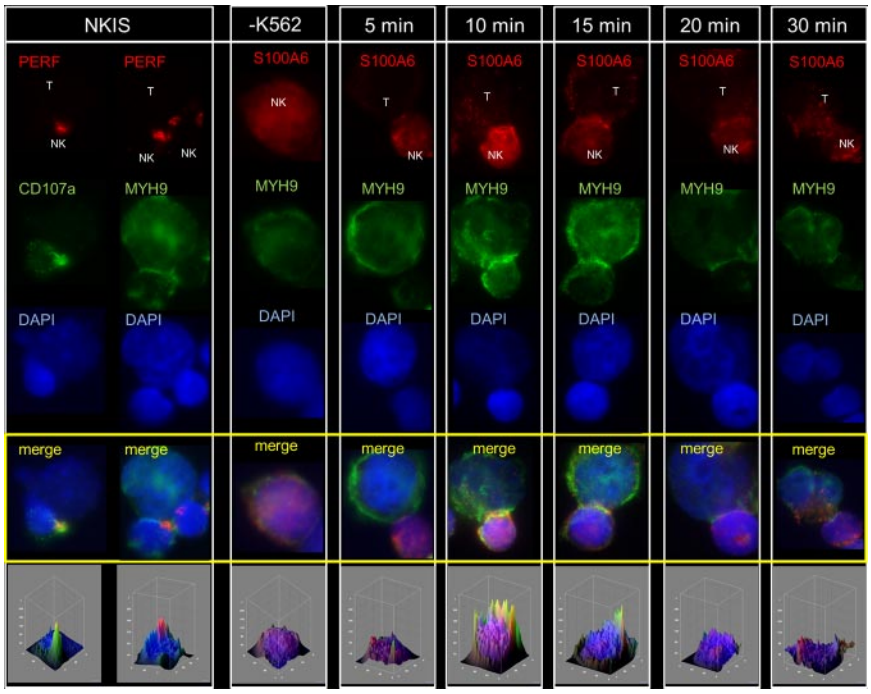

FIG. 7. **Time-resolved colocalization studies of S100A6 and MYH9 in activated NK cells.** NK cells were incubated and activated with K562 target cells ('T' for target cell and "NK" for NK cell) for 5, 10, 15, 20, and 30 min. First two rows show proof of concept colocalization events between Perforin (red) and CD107a (green), and between Perforin (red) and MYH9 (green). Time-resolved activation of NK cells and stain for S100A6 (red) and MYH9 (green) and DNA (DAPI, blue) with appropriate antibodies revealed remarkable time-dependent formation of colocalization events at the NKIS. Anti S100A6 was stained with goat anti-mouse IgG (Alexa 594) and anti-MYH9 (Myosin IIA) with goat anti-rabbit IgG (Alexa 488) supplemented with DAPI (1:1000). Imaging was performed on an inverted microscope (Axiovert 100TV; Carl Zeiss, Jena, Germany) microscope using standard epifluorescence illumination (light source HXP120, Zeiss) and 63×/NA1.4 or 100×/NA1.4 plan-apochromatic objectives. Imaging was performed at room temperature with immersion oil. Images were acquired with a back-illuminated, cooled charge-coupled-device camera (CoolSNAP HQ2, Photometrics, Tucson, AZ, USA) driven by Metamorph software (Version 7.5.3.0; Molecular Devices Corp., Downingtown, PA, USA). Five independent experiments were performed and 20–30 images were acquired per coverslip in each experiment. Image analysis was performed with ImageJ (version 1.44p).

of cytotoxic granules with F-actin for further transport to NKIS (3–5), we were wondering whether S100A4 and S100A6 are involved in these processes. Time-resolved localization studies actually revealed the recruitment of S100A4 and S100A6 together with MYH9 to the NKIS in cytotoxic $CD56^{dim}$ NK cells, with peak levels after 10 and 15 min (see Fig. 6 and Fig. 7). These findings confirm their involvement in NKIS-mediated responses, although their direct functional contribution remains at this time uncharacterized. S100A4 can regulate MYH9 activity (45) and might be an indirect mediator of cytotoxic granule transport.

Further candidates were detected regulated mostly at individual developmental stages, and their functional characterization will likely help to unravel the unique capabilities of distinct NK subsets: The AK1C3 (Aldo-ketoreductase family 1 member C3) converts steroid aldehydes and ketones into alcohols and may play a role in controlling cell growth and/or differentiation. AK1C3 was previously shown to be expressed in NK cells and was also suggested as marker for "healthy and normal" NK cells (53). This proteomic study revealed a subset-specific expression profile for AK1C3 that was detected most abundant in cytotoxic $CD56^{dim}$ NK cells. This suggests AK1C3 as marker for fully functional and cytotoxic NK cells and a role in NK cell effector functions.

On the other hand, FLNB (Filamin B) was exclusively identified in $CD56^{bright}$ NK cells in high amounts. Kanters and colleagues identified the actin cross-linking molecule Filamin B as a novel binding-partner for intracellular adhesion molecule-1 (ICAM-1) and confirmed the ICAM-driven transendothelial migration of leukocytes (54). Thus, Filamin B may be an important mediator of transendothelial migration of $CD56^{bright}$ NK cells from secondary lymphoid tissues (SLO) to peripheral blood during maturation.

In conclusion, results of this study fully support the recent NK cell differentiation model and revealed a limited number of novel donor-independent and subset-specific protein regulations. The systematic inspection of distinct primary NK development stages thereby helps to prioritize candidates such as LEG1, AK1C3, and Filamin B for perspective functional studies. S100A4 and S100A6 most likely are of general importance in NKIS-mediated responses. Following the example of this time-resolved localization studies, single molecule high-resolution imaging may guide us likely to the next molecular hallmarks of NK cell biology.

Acknowledgments—We thank the DFG for funding the IRTG1273 project (Molecular Mechanisms of NK cell cytotoxicity) and the FOR 629 (Tubulin Modifications), the SFB854 for support, the blood bank NSTOB, Springe Germany and especially Prof. Dr. Henk Garritsen for providing us with buffy coats, Undine Felgenträger and Kirsten Minkhart for technical assistance, Christoph Gernert and Thorsten Johl for statistical evaluations in bioinformatics, and Dr. Uwe Kärst for helpful discussions (all HZI).

* To whom correspondence should be addressed: Research Group Cellular Proteomics, Department of Structural Biology, Helmholtz-Centre for Infection Research, Inhoffenstraβe 7, D-38124 Braunschweig, Germany. Tel.: +49 531 6181 3030; Fax: +49 531 6181 7099; E-mail: Lothar.Jaensch@helmholtz-hzi.de.

[S] This article contains supplemental Figs. S1 and S2 and Tables S1 to S8.

AUTHOR CONTRIBUTIONS: Conceived and designed the experiments: MS, SK, MvH, LJ. Sorting of NK cell subsets: LG. Performed the MS-experiments: MS, UL. Performed statistical evaluation: FK. Performed microscopic analysis: MS, BB, MvH. Analyzed the data: MS and UL. Wrote the paper: MS SK LJ.

CONFLICT OF INTEREST DISCLOSURES: The authors Maxi Scheiter, Ulrike Lau, Marco van Ham, Björn Bulitta, Lothar Gröbe, Frank Klawonn, Sebastian König and Lothar Jänsch declare their affiliation to Helmholtz-Zentrum fuer Infektionsforschung GmbH. This does not alter the authors' adherence to all the MCP policies on sharing data and materials.

REFERENCES

1. Lanier, L. L. (2005) NK cell recognition. *Annu. Rev. Immunol.* **23,** 225–274
2. Vivier, E., Tomasello, E., Baratin, M., Walzer, T., and Ugolini, S. (2008) Functions of natural killer cells. *Nat. Immunol.* **9,** 503–510
3. Sanborn, K. B., Rak, G. D., Maru, S. Y., Demers, K., Difeo, A., Martignetti, J. A., Betts, M. R., Favier, R., Banerjee, P. P., and Orange, J. S. (2009) Myosin IIA associates with NK cell lytic granules to enable their interaction with F-actin and function at the immunological synapse. *J. Immunol.* **182,** 6969–6984
4. Sanborn, K. B., Mace, E. M., Rak, G. D., Difeo, A., Martignetti, J. A., Pecci, A., Bussel, J. B., Favier, R., and Orange, J. S. (2011) Phosphorylation of the myosin IIA tailpiece regulates single myosin IIA molecule association with lytic granules to promote NK-cell cytotoxicity. *Blood* **118,** 5862–5871
5. Andzelm, M. M., Chen, X., Krzewski, K., Orange, J. S., and Strominger, J. L. (2007) Myosin IIA is required for cytolytic granule exocytosis in human NK cells. *J. Exp. Med.* **204,** 2285–2291
6. Fehniger, T. A., Cooper, M. A., Nuovo, G. J., Cella, M., Facchetti, F., Colonna, M., and Caligiuri, M. A. (2003) CD56bright natural killer cells are present in human lymph nodes and are activated by T cell-derived IL-2: a potential new link between adaptive and innate immunity. *Blood* **101,** 3052–3057
7. Cooper, M. A., Fehniger, T. A., Turner, S. C., Chen, K. S., Ghaheri, B. A., Ghayur, T., Carson, W. E., and Caligiuri, M. A. (2001) Human natural killer cells: a unique innate immunoregulatory role for the CD56(bright) subset. *Blood* **97,** 3146–3151
8. Freud, A. G., and Caligiuri, M. A. (2006) Human natural killer cell development. *Immunol. Rev.* **214,** 56–72
9. Freud, A. G., Becknell, B., Roychowdhury, S., Mao, H. C., Ferketich, A. K., Nuovo, G. J., Hughes, T. L., Marburger, T. B., Sung, J., Baiocchi, R. A., Guimond, M., and Caligiuri, M. A. (2005) A human CD34(+) subset resides in lymph nodes and differentiates into CD56bright natural killer cells. *Immunity* **22,** 295–304
10. De Maria, A., Bozzano, F., Cantoni, C., and Moretta, L. (2011) Revisiting human natural killer cell subset function revealed cytolytic CD56(dim)CD16+ NK cells as rapid producers of abundant IFN-gamma on activation. *Proc. Natl. Acad. Sci. U.S.A.* **108,** 728–732
11. Poli, A., Michel, T., Thérésine, M., Andrès, E., Hentges, F., and Zimmer, J. (2009) CD56bright natural killer (NK) cells: an important NK cell subset. *Immunology* **126,** 458–465
12. Chan, A., Hong, D. L., Atzberger, A., Kollnberger, S., Filer, A. D., Buckley, C. D., McMichael, A., Enver, T., and Bowness, P. (2007) CD56bright human NK cells differentiate into CD56dim cells: role of contact with peripheral fibroblasts. *J. Immunol.* **179,** 89–94
13. Jaeger, B. N., Donadieu, J., Cognet, C., Bernat, C., Ordoñez-Rueda, D., Barlogis, V., Mahlaoui, N., Fenis, A., Narni-Mancinelli, E., Beaupain, B., Bellanné-Chantelot, C., Bajénoff, M., Malissen, B., Malissen, M., Vivier, E., and Ugolini, S. (2012) Neutrophil depletion impairs natural killer cell maturation, function, and homeostasis. *J. Exp. Med.* **209,** 565–580
14. Romagnani, C., Juelke, K., Falco, M., Morandi, B., D'Agostino, A., Costa, R., Ratto, G., Forte, G., Carrega, P., Lui, G., Conte, R., Strowig, T., Moretta, A., Münz, C., Thiel, A., Moretta, L., and Ferlazzo, G. (2007) CD56brightCD16- killer Ig-like receptor- NK cells display longer telomeres and acquire features of CD56dim NK cells upon activation. *J. Immunol.* **178,** 4947–4955
15. Björkström, N. K., Riese, P., Heuts, F., Andersson, S., Fauriat, C., Ivarsson, M. A., Björklund, A. T., Flodström-Tullberg, M., Michaëlsson, J., Rottenberg, M. E., Guzmán, C. A., Ljunggren, H. G., and Malmberg, K. J. (2010) Expression patterns of NKG2A, KIR, and CD57 define a process of CD56dim NK-cell differentiation uncoupled from NK-cell education. *Blood* **116,** 3853–3864
16. Hong, H. S., Eberhard, J. M., Keudel, P., Bollmann, B. A., Ballmaier, M., Bhatnagar, N., Zielinska-Skowronek, M., Schmidt, R. E., and Meyer-Olson, D. (2010) HIV infection is associated with a preferential decline in less-differentiated CD56dim CD16+ NK cells. *J. Virol.* **84,** 1183–1188
17. Béziat, V., Descours, B., Parizot, C., Debré, P., and Vieillard, V. (2010) NK cell terminal differentiation: correlated stepwise decrease of NKG2A and acquisition of KIRs. *PloS One.* **5,** e11966
18. Lopez-Vergès, S., Milush, J. M., Pandey, S., York, V. A., Arakawa-Hoyt, J., Pircher, H., Norris, P. J., Nixon, D. F., and Lanier, L. L. (2010) CD57 defines a functionally distinct population of mature NK cells in the human CD56dimCD16+ NK-cell subset. *Blood* **116,** 3865–3874
19. Abo, T., Miller, C. A., and Balch, C. M. (1984) Characterization of human granular lymphocyte subpopulations expressing HNK-1 (Leu-7) and Leu-11 antigens in the blood and lymphoid tissues from fetuses, neonates and adults. *Eur. J. Immunol.* **14,** 616–623
20. Brodin, P., Lakshmikanth, T., Johansson, S., Kärre, K., and Höglund, P. (2009) The strength of inhibitory input during education quantitatively tunes the functional responsiveness of individual natural killer cells. *Blood* **113,** 2434–2441
21. Joncker, N. T., Fernandez, N. C., Treiner, E., Vivier, E., and Raulet, D. H. (2009) NK cell responsiveness is tuned commensurate with the number of inhibitory receptors for self-MHC class I: the rheostat model. *J. Immunol.* **182,** 4572–4580
22. Sun, J. C., Beilke, J. N., and Lanier, L. L. (2009) Adaptive immune features of natural killer cells. *Nature* **457,** 557–561
23. Lopez-Vergès, S., Milush, J. M., Schwartz, B. S., Pando, M. J., Jarjoura, J., York, V. A., Houchins, J. P., Miller, S., Kang, S.-M., Norris, P. J., Nixon, D. F., and Lanier, L. L. (2011) Expansion of a unique CD57$^+$NKG2Chi natural killer cell subset during acute human cytomegalovirus infection. *Proc. Natl. Acad. Sci. U.S.A.* **108,** 14725–14732
24. Björkström, N. K., Lindgren, T., Stoltz, M., Fauriat, C., Braun, M., Evander, M., Michaëlsson, J., Malmberg, K. J., Klingström, J., Ahlm, C., and Ljunggren, H. G. (2011) Rapid expansion and long-term persistence of elevated NK cell numbers in humans infected with hantavirus. *J. Exp. Med.* **208,** 13–21
25. Petitdemange, C., Becquart, P., Wauquier, N., Béziat, V., Debré, P., Leroy, E. M., and Vieillard, V. (2011) Unconventional repertoire profile is imprinted during acute chikungunya infection for natural killer cells polarization toward cytotoxicity. *PLoS Pathog.* **7,** e1002268
26. Björkström, N. K., Svensson, A., Malmberg, K. J., Eriksson, K., and Ljunggren, H. G. (2011) Characterization of natural killer cell phenotype and function during recurrent human HSV-2 infection. *PloS One* **6,** e27664
27. Sun, J. C., Madera, S., Bezman, N. A., Beilke, J. N., Kaplan, M. H., and Lanier, L. L. (2012) Proinflammatory cytokine signaling required for the generation of natural killer cell memory. *J. Exp. Med.* **209,** 947–954
28. Rakkola, R., Matikainen, S., and Nyman, T. A. (n.d.). Proteome characterization of human NK-92 cells identifies novel IFN-alpha and IL-15 target genes. *J Proteome Res.* **4,** 75–82
29. Liu, X. C., Liang, H., Tian, Z., Ruan, Y. S., Zhang, L., and Chen, Y. (2007) Proteomic analysis of human NK-92 cells after NK cell-mediated cyto-

toxicity against K562 cells. *Biochemistry* **72,** 716–727
30. Hanna, J., Fitchett, J., Rowe, T., Daniels, M., Heller, M., Gonen-Gross, T., Manaster, E., Cho, S. Y., LaBarre, M. J., and Mandelboim, O. (2005) Proteomic analysis of human natural killer cells: insights on new potential NK immune functions. *Mol Immunol.* **42,** 425–431
31. Ghosh, D., Lippert, D., Krokhin, O., Cortens, J. P., and Wilkins, J. A. (2010) Defining the membrane proteome of NK cells. *J Mass Spectrom.* **45,** 1–25
32. Van Damme, P., Maurer-Stroh, S., Plasman, K., Van Durme, J., Colaert, N., Timmerman, E., De Bock, P.-J., Goethals, M., Rousseau, F., Schymkowitz, J., Vandekerckhove, J., and Gevaert, K. (2009) Analysis of protein processing by N-terminal proteomics reveals novel species-specific substrate determinants of granzyme B orthologs. *Mol. Cell. Proteomics* **8,** 258–272
33. König, S., Nimtz, M., Scheiter, M., Ljunggren, H.-G., Bryceson, Y. T., and Jänsch, L. (2012) Kinome analysis of receptor-induced phosphorylation in human natural killer cells. *PLoS One* **7,** e29672
34. Sitnicka, E. (2011) Early cellular pathways of mouse natural killer cell development. *J. Innate Immun.* **3,** 329–336
35. Wessel, D., and Flügge, U. I. (1984) A method for the quantitative recovery of protein in dilute solution in the presence of detergents and lipids. *Anal. Biochem.* **138,** 141–143
36. Klawonn F. (2012) Significance tests to identify regulated proteins based on a large number of small samples. *Kybernetica* **48,** 478–493
37. Wendt, K., Wilk, E., Buyny, S., Buer, J., Schmidt, R. E., and Jacobs, R. (2006) Gene and protein characteristics reflect functional diversity of CD56dim and CD56bright NK cells. *J. Leukoc. Biol.* **80,** 1529–1541
38. Sedelies, K. A., Sayers, T. J., Edwards, K. M., Chen, W., Pellicci, D. G., Godfrey, D. I., and Trapani, J. A. (2004) Discordant regulation of granzyme H and granzyme B expression in human lymphocytes. *J. Biol. Chem.* **279,** 26581–26587
39. Persic, V., Ruzic, A., Miletic, B., Samsa, D. T., Rakic, M., Raljevic, D., Pejčinović, V. P., Eminovic, S., Zaputovic, L., and Laskarin, G. (2012) Granulysin Expression in Lymphocytes that Populate the Peripheral Blood and the Myocardium After an Acute Coronary Event. *Scan. J. Immunol.* **75,** 231–242
40. Sague, S. L., Tato, C., Puré, E., and Hunter, C. A. (2004) The regulation and activation of CD44 by natural killer (NK) cells and its role in the production of IFN-gamma. *J. INterferon Cytokine Res.* **24,** 301–309
41. Márquez, C., Trigueros, C., Fernández, E., and Toribio, M. L. (1995) The development of T and non-T cell lineages from CD34+ human thymic precursors can be traced by the differential expression of CD44. *J. Exp. Med.* **181,** 475–483
42. Koopman, L. A., Kopcow, H. D., Rybalov, B., Boyson, J. E., Orange, J. S., Schatz, F., Masch, R., Lockwood, C. J., Schachter, A. D., Park, P. J., and Strominger, J. L. (2003) Human decidual natural killer cells are a unique NK cell subset with immunomodulatory potential. *J. Exp. Med.* **198,** 1201–1212
43. Stoeckle, C., Gouttefangeas, C., Hammer, M., Weber, E., Melms, A., and Tolosa, E. (2009) Cathepsin W expressed exclusively in CD8+ T cells and NK cells, is secreted during target cell killing but is not essential for cytotoxicity in human CTLs. *Exp Hematol.* **37,** 266–275
44. Takenaga, K., Nakamura, Y., Sakiyama, S., Hasegawa, Y., Sato, K., and Endo, H. (1994) Binding of pEL98 protein, an S100-related calcium-binding protein, to nonmuscle tropomyosin. *J. Cell Biol.* **124,** 757–768
45. Kriajevska, M. V., Cardenas, M. N., Grigorian, M. S., Ambartsumian, N. S., Georgiev, G. P., and Lukanidin, E. M. (1994) Non-muscle myosin heavy chain as a possible target for protein encoded by metastasis-related mts-1 gene. *J. Biol. Chem.* **269,** 19679–19682
46. Liu, D., Bryceson, Y. T., Meckel, T., Vasiliver-Shamis, G., Dustin, M. L., and Long, E. O. (2009) Integrin-dependent organization and bidirectional vesicular traffic at cytotoxic immune synapses. *Immunity* **31,** 99–109
47. Moretta, L. (2010) Dissecting CD56dim human NK cells. *Blood* **116,** 3689–3691
48. Bryceson, Y. T., Fauriat, C., Nunes, J. M., Wood, S. M., Björkström, N. K., Long, E. O., and Ljunggren, H. G. (2010) Functional analysis of human NK cells by flow cytometry. *Methods Mol. Biol.* **612,** 335–352
49. Bryceson, Y. T., March, M. E., Ljunggren, H. G., and Long, E. O. (2006) Activation, coactivation, and costimulation of resting human natural killer cells. *Immunol. Rev.* **214,** 73–91
50. Garín, M. I., Chu, C. C., Golshayan, D., Cernuda-Morollón, E., Wait, R., and Lechler, R. I. (2007) Galectin-1: a key effector of regulation mediated by CD4+CD25+ T cells. *Blood* **109,** 2058–2065
51. Cedeno-Laurent, F., and Dimitroff, C. J. (2012) Galectin-1 research in T cell immunity: past, present and future. *Clin. Immunol.* **142,** 107–116
52. Jeon, C. H., Kim, H. L., and Park, J. H. (2009) Induction of S100A4, S100A6, and galectin-1 during the lineage commitment of CD4+CD8+ thymocyte cell line is suppressed by 2,3,7,8-tetrachlorodibenzo-p-dioxin. *Toxicol. Lett.* **187,** 157–163
53. Choi, Y. L., Makishima, H., Ohashi, J., Yamashita, Y., Ohki, R., Koinuma, K., Ota, J., Isobe, Y., Ishida, F., Oshimi, K., and Mano, H. (2004) DNA microarray analysis of natural killer cell-type lymphoproliferative disease of granular lymphocytes with purified CD3-CD56+ fractions. *Leukemia* **18,** 556–565
54. Kanters, E., van Rijssel, J., Hensbergen, P. J., Hondius, D., Mul, F. P., Deelder, A. M., Sonnenberg, A., van Buul, J. D., and Hordijk, P. L. (2008) Filamin B mediates ICAM-1-driven leukocyte transendothelial migration. *J. Biol. Chem.* **283,** 31830–31839